Improving the Performance of a Realistic Distribution Network in Kirkuk by Integrating a Distributed Hybrid System

Hashim K. Ahmed*‡, R. Nejat TUNCAY*, Mohammed H. Alkhafaji**

*Department of Electrical and Electronics Engineering, Faculty of Engineering and Natural Sciences, Istanbul Okan University, Istanbul 34959, Turkey

** Department of Electrical Engineering, University of Technology, Baghdad, Iraq

(haahmed@stu.okan.edu.tr, nejat.tuncay@okan.edu.tr, Mohammed.h.alkhafaji@uotechnology.edu.iq)

‡ Corresponding Author; Hashim K. Ahmed, Kirkuk-Iraq 36001, Tel: +9647702324913, haahmed@stu.okan.edu.tr

Received: 28.03.2023 Accepted:11.05.2023

Abstract- This study determines the causes and possible solutions to an actual problem suffers due to the distribution network of Al-Shajara village, a rural feeder in Kirkuk, north of Iraq. It is a radial distribution system with an approximate length of 27 km and is distributed with a system voltage of 11 kV. Consequently, the consumers fed through this feeder are getting excessive voltage drops together with line losses and frequent outages in the power supply. The research works to build a hybrid system of Distributed Generation (DG) based on renewable energies available in the study area are solar energy, hydropower and batteries to cover the energy demand and improve system performance. Moreover, Open Distribution System Simulator (OpenDSS) software connected to MATLAB via an OpenDSS COM server is used to analyze the power flow in the distribution system, while AotoAdd optimization technology is also used to determine the optimal location for the integration of Distributed Generators (DGs) and Shunt Capacitors (SCs). The simulations of the proposed system have been carried out under three different loads according to two scenarios which are the connected mode and the island mode. The results demonstrated the effectiveness of the proposed techniques as well as improved the voltage profile to be within the standard limits in all buses, greater than 0.95 pu and less than 1.05 pu. Furthermore, the percentage reduction of power losses has reached 97% at full load. Additionally, the results proved that the island mode is superior to the connected mode.

Keywords Distributed generation, optimization, renewable PV/mini-hydro/battery system, grid supplemented or stand alone, OpenDSS & AutoAdd software.

1. Introduction

In recent decades, work has accelerated in the field of developing renewable energy resources to create promising sources in building an environmentally friendly and sustainable energy economy. One of the most important concepts on which focus has increased within the concepts of renewable energies is the concept of distributed generation. DG refers to any technology for producing electric power that is integrated within the distribution system, and close to the point of use [1]. DG systems in general and systems based on renewable energy resources in particular are of great interest, due to their contribution to the field of energy security by reducing dependence on fossil fuels and reducing greenhouse gases [2]. DG integration with distribution systems achieves environmental, economic and technical benefits. Reducing dependence on fossil fuels, lower system costs, and lower electricity prices are environmental and economic benefits. Also the voltage profile Optimizing, reducing losses, power quality and increasing system reliability are technical benefits [3]. DG technology is a suitable solution to the shortage of electric power supply and contributes to the stability of distribution systems, is the basis and nucleus of micro-grids and smart grids [4]. Moreover, DG can work independently to secure demand for the local consumer, is called isolated systems. Also, DG can be connected to the public electrical network to contribute part of the energy demand, is called grid-connected systems. Electricity companies usually suffer from the difficulty of

supplying electricity to remote areas, due to cost of transmission lines, distribution stations in addition to energy losses. At the same time, subscribers in those areas suffer from poor power quality and frequent power outages. Recently, the focus has increased on securing electricity for these areas from distributed generation systems, especially from systems that depend on renewable energies such as wind energy, solar energy, small hydroelectric stations, and others. However, weather fluctuations make the output of renewable energy systems unstable and limit their production. Therefore, a Hybrid Renewable Energy System (HRES) by combining several renewable energies resources is a promising solution to this problem [5, 6]. Hybrid systems are important for several of reasons, the most crucial of which is ensuring the continuity of feeding the load with electrical energy under various operating conditions and making the optimal use of the resources for renewable energies available [7]. In addition to the economic factor, which is important because using a hybrid system is much less expensive than using a single- mode generation system [8, 9].

In this research, the resources available in the study area are used and a hybrid photovoltaic PV/hydropower/battery system is formed to cover the energy demand and solve the problems that the 11 kV medium voltage network suffers from: voltage drop, high power loss and frequent power outages. SCs have also been added to the hybrid system for their importance in improving voltage and power factor and reducing power losses. Integration of DGs and SCs with distribution networks will increase reliability, reduce losses and improve power quality, but the optimal location and size must be chosen, to maximize benefits and avoid negative effects [10]. In the past decades many algorithms and optimization techniques with different goals have been proposed for the optimization of DGs and SCs. These techniques include Artificial Bee Colony (ABC), elephant grazing optimization (EHO), Genetic Algorithm (GA), Shuffled Frog Leap Algorithm (SFLA), Particle Swarm Optimization (PSO) along with other local and global search methods etc. ; also, some authors have used PSO technique to optimize and manage energy in hybrid electric vehicles [11, 12]. The authors in [13] proposed intelligent allocation of distributed generating units DGs and shunt reactive compensators with high penetration capabilities in distribution systems to enhance voltage stability and mitigate power loss using the "Bald Eagle Search BES" optimization technique. While [14] an Ant Colony Optimization (ACO) algorithm for optimal integration of DG into the distribution system to reduce the Technical Economic Objective Function (TEOF) is discussed. Another research [15] presented a highly effective method for installing both capacitors and photovoltaic systems in distribution systems in order to reduce total energy loss in branches using the "Stochastic Fractal Search Optimization Algorithm (SFSOA)". The research also shows the real impact of utilizing both photovoltaic systems and capacitors to minimize active power losses and enhance the voltage profile of distribution systems.

The [16], a concrete case study of the effect of connecting a mini-power station of a hybrid PV wind turbine to a rural LV power grid was simulated using PJ-elec software, in order to compensate for the fault point voltage. While [17] used "Binary Particle Swarm Optimization and Shuffled Frog Leap (BPSO-SFLA) algorithms" to simulate and test the Optimal Power Flow (OPF) on the distribution system and to detect the optimal location and size of DGs. Where the result shows that the algorithms improve voltage stability, provide better dynamic decors distribution and reduce energy losses, but in the initial stage of progress. Other researchers in [18] proposed a Modified Moth Flame Optimization (MMFO) algorithm; to find the optimal location and size of DG units based on renewable energy sources in the distribution system, in order to minimize the total active power loss and bus voltage deviation. Furthermore, in [10] the optimal location and size of distributed generators in distribution network was obtained using performance indicators related to voltage stability, power loss, substation power consumption and short-circuit current deviation. The optimization was performed using "particle swarm optimization and chaotic particle swarm" optimization algorithms.

[19] Proposed a new plan based on an enhanced technique to identify the optimum location, size, and power factor of DG units to be integrated with distribution networks to achieve max DG penetration. It is the "Quasi-Oppositional Chaotic Symbiotic Organisms Search (QOCSOS)" technique, an upgraded version of the original (SOS) algorithm, is the proposed meta method. Additionally, [20] proposed a new hybrid technology for optimal allocation of photovoltaic generations and wind turbines (PV and WT), are Fuzzy Logic Controller (FLC) and Ant-Lion Optimization Algorithm (ALOA) with Particle Swarm Optimization (PSO) based group. With the aim of improving voltage stability and reducing loss. In [21], an analytical optimization method was developed and a new methodology for optimal investment in DG developed, based on the optimal allocation of DG units and integrated capacitors to mitigate network voltage limitations and reduce the cost of interconnection for the integration of renewable energy generation in medium voltage public distribution networks. Although these algorithms are known and effective for solving a variety of DG mapping problems, they have certain drawbacks, such as the possibility of becoming stuck in local minima, slow convergence, and time-consuming implementation for specific problems. Inconsistencies in exploration and exploitation, duplication of search strategies, difficulty in determining appropriate parameter values to determine the optimal solution, and other issues lead to these problems. In this study the AutoAdd algorithm is used to find the optimal solutions by locating the DGs and SCs based on OpenDSS interfaced with MATLAB via the OpenDSS COM server [22, 23]. AutoAdd is a mode and function of OpenDSS, used to study optimal locations of capacitors and generators to improve the voltage profile and reduce network power losses.

2. Methods and Models

2.1. Power Flow Analysis

All In this research the Open Distribution System Simulator (OpenDSS), an open-source simulation engine for electrical power systems, was employed to resolve the power flow using the Matlab coding interface and to acquire information about the power system, including power losses, voltage profiles, the active and reactive power flowing through each line, etc. [24, 25]. The iterative technique is adopted to solve the power flow using the normal mode solve algorithm is a simple fixed point iterative method and works well for almost all distribution systems [22]. The Fig.1 shows the algorithm's iterative principle. The Power Conversion (PC) component of the OpenDSS is described according to Fig.2. PC elements are considered as Norton Equivalents to represent nonlinear parts such as the generator and load, with a constant admittance matrix *Yprim* and an injection current *Ipc* (*inj*) to compensate the nonlinear component. The admittance matrix for the system is built using the admittance matrices of each constituent. The algorithm procedure as follows [23, 26-30]:

1- Clear all PC components from the network, and calculate the system's initial node voltage value (V_0) utilizing the network admittance matrix.

2- Include every PC component in the network, calculate each PC element's injection current (I_{inj}) using its admittance matrix, power and node voltage.

3- Create an injection current matrix using the injection currents from each PC component. Through matrix operation, node voltages can be determined using the injection current matrix and the system admittance matrix.

4- Where the system node voltage value is corrected continually throughout the iterative process until the convergence of 0.0001 pu is reached. Fig.3 is an illustrative diagram that summarizes the steps of the algorithm.

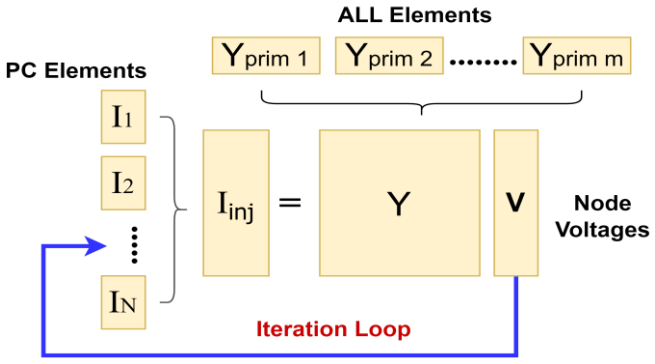

Fig. 1. Power flow solution loop of OpenDSS [22, 23, 27].

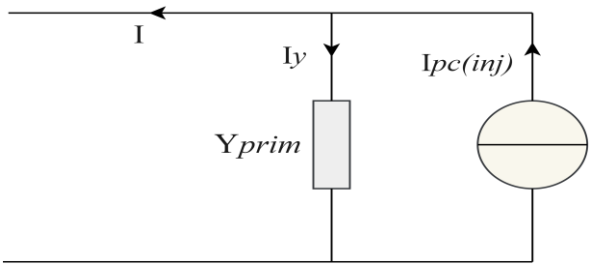

Fig. 2. PC element model of OpenDSS [26].

2.2. Optimization Algorithm

In this study, an AutoAdd algorithm is used to find the optimal solutions by locating the DGs and SCs with the help of OpenDSS interfaced with MATLAB via the OpenDSS COM server. AutoAdd mode is an internal feature of OpenDSS to reduce losses and improve voltage profile [31]. The optimization problem of distribution system is shown in equation below [32].

$$Min\ f(x,y) = P_{loss} \quad (1)$$

$$Subject - to\ g\ (x,y) = 0$$

$$0.95 \leq Vi \leq 1.05$$

Where, g (x, y) = 0 is the Equation of Distribution Power Flow, x: Active power, y: Reactive power, P_{loss}: Power losses, Vi: Voltage at *ith* bus.

The amount of power that is injected to each bus in order to keep the voltage within the specified limits and to reduce system losses is determined by Eq. (1). Since OpenDSS uses an iterative method to look for unknown voltages and currents, AutoAdd mode benefits from direct access to the compensation current matrix during the solution [32]. In order to transfer a DG or SC from one bus to another, it only requires alteration in the current compensation matrix. Additionally, this algorithm's solution convergence velocity rises as a result of the system's admission matrix remaining constant. The results are displayed as a percentage factor of each vector, and the method to locate each generator or capacitor typically requires 2-4 iterations (in each solution). Where the next-best power supply is located is indicated by the Improvement Factor percentage. The AutoAdd optimization approach to reducing losses is depicted in Fig. 4.

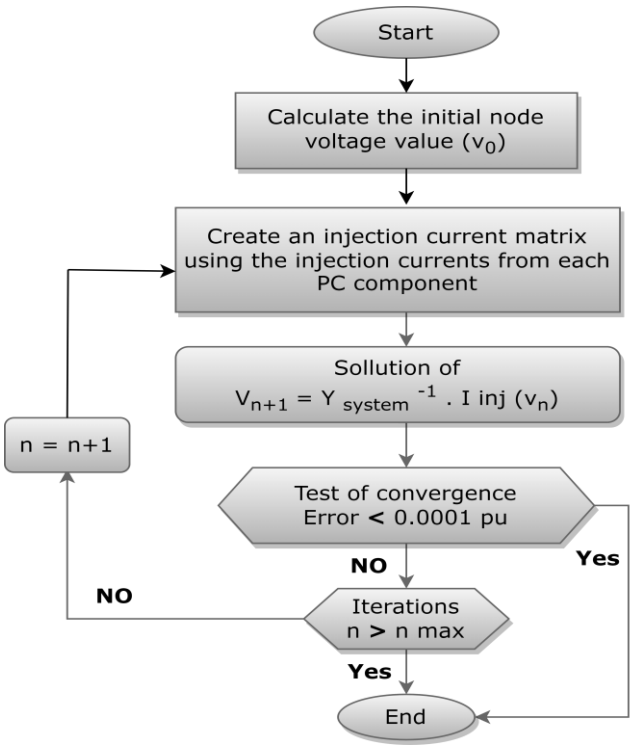

Fig. 3. Flowchart of the iterative technique.

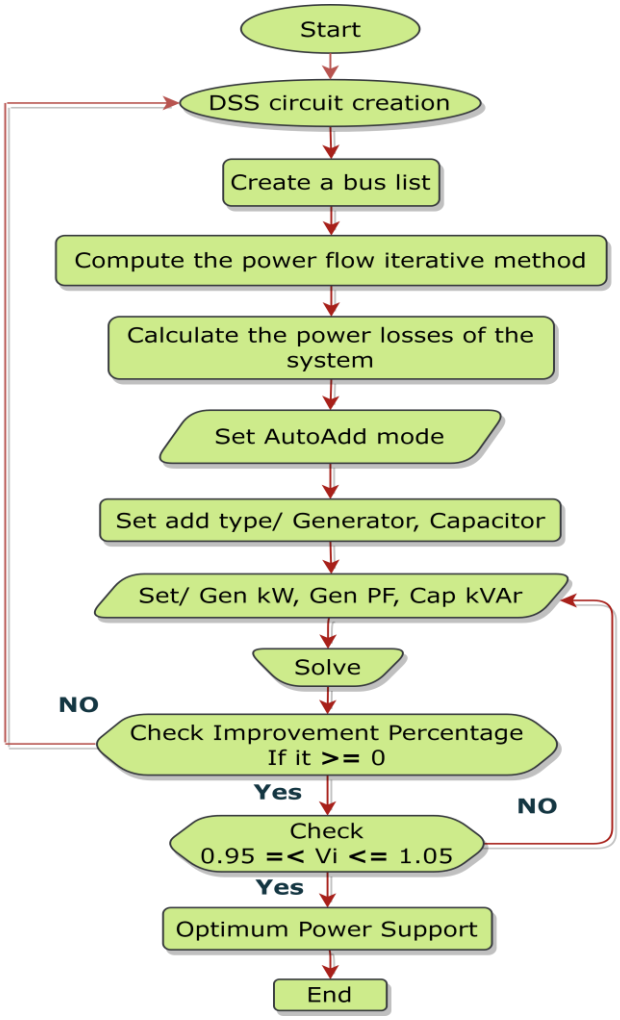

Fig. 4. AutoAdd algorithm basic flowchart.

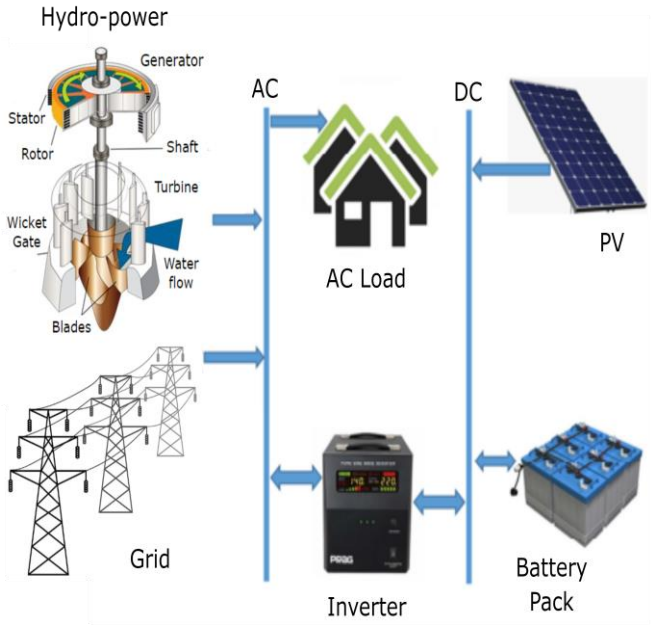

Fig. 5. Configuration of hybrid energy system PV/hydro/battery.

2.3. Photovoltaic System

The power generated by the photovoltaic system at each moment depends mainly on the intensity of radiation at that moment. Also, high temperatures have a negative impact on the performance of the PV system. The output power can be formulated as follows [33-37]:

$$P_{ph}(t) = P_{STC} \times \frac{G(t)}{G_{STC}} [1 + Kp\,(T(t) - T_{STC})] \quad (2)$$

Where G_{STC} and T_{STC} are the solar radiation and temperature of the PV module under STC conditions. G (t) and T (t) are the actual solar radiation and cell temperatures at time t. P_{ph} (t) is the available DC power at time t, and P_{STC} denotes the PV module's output power under STC Conditions. Kp is a coefficient that expresses the power reduction due to the temperature rise of the PV array.

To calculate the solar module temperature (T) the following linear model is used [35, 36, 38, 39]:

$$T = T_a + \frac{G}{G_{NOCT}} \times (T_{NOCT} - 20) \quad (3)$$

Where T is PV cell temperature, T_{NOCT} is a nominal cell operating temperature given by the manufacturer (℃), Ta is an ambient temperature (℃), G_{NOCT} is a solar radiation intensity of 800 W/m^2, and G is measured solar radiation intensity at the particular time in W/m^2.

2.4. Hydropower Plant (HPP)

The choice of turbine size depends on the net head and the maximum water flow rate, which must be determined by the river or stream in which the turbine is to be installed. In this research, we assume the installation of two mini hydroelectric turbines (2×1500 kW) on Makhoul Dam, which is a dam under construction on the Tigris River and located near the study area [40-42]. The water flow rate through the turbine (Q) in winter was evaluated as 5 m^3/s per turbine, minimum flow rate in summer 4 m^3/s per turbine and net head (H) 40 m. The electrical generated power can be calculated using the following equation [43-47]:

$$P_{hydro}\ (kW) = \frac{\eta \times \rho \times g \times Q \times H}{1000} \quad (4)$$

Where η is the overall efficiency of the hydropower system, is set as 80%, ρ is the density of water ($1000\ kg/m^3$), g is the acceleration due to gravity (9.81 m/s^2).

2.5. Battery

Solar and hydro resources have intermittent energy output and as such, an energy storage system like a battery is required to balance its fluctuations and to meet the lack of energy quantity at peak hours. Battery size is calculated by [8, 48]:

$$C_{Bat} = \frac{E_R \times AD}{DOD \cdot V \cdot \eta_{Inv} \cdot \eta_{Batt}} \quad (5)$$

Where E_R is the energy required and V is system voltage. Battery efficiency (η_{Batt}), inverter efficiency (η_{inv}), depth of

discharge (*DOD*), autonomy days (*AD*) are set as 0.95, 0.98, 80% and 1 respectively.

Power fluctuations of renewable energy sources are managed by charging and discharging batteries for continuous load supply. The energy flow during charging and discharging of the battery can be calculated as follows [49-51]:

- Battery charging mode

$$E_{Batt}(t) = E_{Batt}(t-1)(1-\delta) + \left(E_{PV}(t) + \left(E_{hydro}(t) - E_{load}(t)\right) \times \eta_{Inv}\right) \times \eta_{Batt,ch}$$
$$, \left(E_{PV}(t) + E_{hydro}(t)\right) > E_{load}(t) \quad (6)$$

- Battery discharging mode

$$E_{Batt}(t) = E_{Batt}(t-1)(1-\delta) - \left(\left(\frac{E_{load}(t) - E_{hydro}(t)}{\eta_{Inv}}\right) - E_{PV}(t)\right) \div \eta_{Batt,disch}$$
$$, \left(E_{PV}(t) + E_{hydro}(t)\right) < E_{load}(t) \quad (7)$$

Where E_{Batt} (t) is Battery energy level at time t and E_{PV} (t), E_{hydro} (t) are energy generated by PV and hydroelectric turbines at time t. δ is the self-discharge rate of battery.

2.6. Shunt Capacitor (SC)

SC units only provide reactive power to distribution systems, and the following equations represent the power loss and voltage drop after adding a capacitor of capacity Q_C [15]:

$$P_{loss} = R \times \left(\frac{P^2 + (Q - Q_C)^2}{V^2}\right) \quad (8)$$

$$Q_{loss} = X \times \left(\frac{P^2 + (Q - Q_C)^2}{V^2}\right) \quad (9)$$

$$VD = \frac{RP + X(Q - Q_C)}{V} \quad (10)$$

The key advantages of DG/SC units in distribution networks are enhanced voltage profile, reduced total power losses, reduced maintenance and operating costs of system, free up capacity of system and improved power stability and dependability [52, 53]. However, appropriate sizes should be chosen and installed in optimal locations.

3. Formulation of Optimization Problem

In general, radial distribution systems (RDS) have a high R/X ratio compared to transmission systems. It suffers from many problems, chief among which are high power losses, low voltage levels, and unreliability. This study aims to minimize the total losses of a realistic distribution network, while enhancing the margin of voltage stability and the voltage profile by selecting the appropriate sizes and optimal locations of DGs and SCs to be installed in RDS using the proposed methodology.

3.1. Objective Function

The main objective of this study is to reduce the overall power loss of radial distribution systems (RDS), while optimizing the voltage level at each bus. Mathematically this objective function is given below:

$$f_{opj} = \min(P_{loss}) + \min(V_{drop}) \quad (11)$$

The power loss for any branch (P_{br}) located between two n, m buses on the network can be calculated as follows [54]:

$$P_{br} = I_{br}^2 \times R_{br} \quad (12)$$

$$Q_{br} = I_{br}^2 \times X_{br} \quad (13)$$

Where I_{br} is the brunch current, R_{br} and X_{br} are the resistance and reactance of Each branch.

Branch current is calculated using the power flow through the branch:

$$I_{br} = \left(\frac{P_n + jQ_n}{V_n}\right)^* \quad (14)$$

From Equations (12), (13) and (14), the power loss of the branch are:

$$P_{loss}(n,m) = \frac{P_n^2 + Q_n^2}{|V_n^2|} \times R_{n,m} \quad (15)$$

$$Q_{loss}(n,m) = \frac{P_n^2 + Q_n^2}{|V_n^2|} \times X_{n,m} \quad (16)$$

The conjugate process is represented by the star. Where P_n and Q_n are the active and reactive Power flow in the branch. *Vn* is receiving end voltage of branch. The system's overall power loss is as follows:

$$P_{loss} = \sum_{i=1}^{N_{br}} P_{br,i} \quad (17)$$

$$Q_{loss} = \sum_{i=1}^{N_{br}} Q_{br,i} \quad (18)$$

Where N_{br} is the system's total number of branches. Total voltage deviation (TVD) measures the difference between the system voltage and the reference Voltage 'unity'. Typically, the TVD is determined as [13, 54]:

$$\text{TVD} = \sum_{i=1}^{N_b} |1 - |V_i|| \quad (19)$$

Where N_b represent number of buses in system and *Vi* is the voltage at *ith* bus.

3.2. Performance Parameters Calculation

This study calculates the performance parameters for each case study of the DG/SC unit allocations. Among these parameters are the active power loss (P_{loss}), the reactive loss (Q_{loss}), and the TVD. To assess the system performance after integrating different compensators, the percentage reductions for the performance parameters in comparison to the base case (without DG/SC integration) are calculated. The decrease in power loss is determined by:

$$\Delta P_{loss} = \frac{P_{loss}^{Base} - P_{loss}^{Comp}}{P_{loss}^{Base}} \times 100 \quad (20)$$

Where the real power losses without and with a compensating device (DG or SC), are represented by P_{loss}^{Base} and P_{loss}^{Comp} respectively. Similar to this, the reactive power loss reduction as a percentage is:

$$\Delta Q_{loss} = \frac{Q_{loss}^{Base} - Q_{loss}^{Comp}}{Q_{loss}^{Base}} \times 100 \quad (21)$$

Where the reactive Power losses without and with a compensating device (DG or SC), are represented by Q_{loss}^{Base} and Q_{loss}^{Comp} respectively. Finally, the TVD's percentage reduction is determined as follows:

$$\Delta TVD = \frac{TVD^{Base} - TVD^{Comp}}{TVD^{Base}} \times 100 \quad (22)$$

Where TVD^{Base} is the total voltage deviation at base case, and TVD^{Comp} is the total voltage deviation after compensating DG or SC.

3.3. Formulation of Constraint

Loads operation, including residential and industrial clients, is directly and severely impacted by the power quality of distribution networks, particularly in industries with highly sensitive production lines and technological equipment. As a result, the operating parameters of the power system, also known as power system operating constraints and physical limits, should be maintained within typical ranges. These distribution network limit criteria can be summed up as follows:

3.3.1. Constraint of Current

Depending on the type of material used and the size of the cross section, each power line has a different carrying capacity. The protective relay can be affected and cut off the power supply due to the overload condition and may also cause damage to the line structure. As shown in the following inequality constraint, the maximum allowable current must be set for each power line to ensure the normal condition of the lines:

$$I_l^{max} \geq I_l ; \quad l = 1, \ldots\ldots, Nl \quad (23)$$

3.3.2. Constraint of Voltage

One of the most crucial factors affecting the power quality of distribution networks is voltage limitation. Electric equipment would malfunction or perform wrongly if the supply voltage of nodes was below or outside of the authorized working range. Therefore, the following voltage restriction in the distribution networks needs to be carefully monitored:

$$U_m^{min} \leq U_m \leq U_m^{max} ; \quad m = 1, \ldots\ldots, Nm \quad (24)$$

Where U_m is the *mth* node's working voltage, U_m^{min} and U_m^{max} are its min and max working voltages; 0.95 and 1.05 pu respectively [13].

3.3.3. Constraints of Reactive Power

To minimize the reactive power derived from the power source of the utility grid, capacitors with reactive power are injected into distribution network nodes. As a result, it lowers the currents in distribution lines and the network's power loss. The power loss is reduced with increasing capacitor capacity; however, the total reactive power injected into the network must not be so high as to exceed the total reactive demand, as this could render the compensatory strategy useless. The combined installed reactive Power of the DG and SC units must never exceed the totally reactive demand of system, as:

$$\{\sum_{k=1}^{N_{DG}} Q_{DG,k} + \sum_{k=1}^{N_{SC}} Q_{SC,k}\} \leq Q_D \quad (25)$$

Where N_{DG}, N_{SC} denotes the number of the DG and SC devices, and Q_{DG}, Q_{SC} denotes the DG and SC installed reactive Power; Q_D is total reactive demand.

3.3.4. Rates of Battery Charging and Discharging

The battery physical Constraints are defined in the Equation (26), for each Hour (h). The hourly State of Charge $SOC_{B,h}$ cannot exceed the max Capacity K_B^{max}, and it has to be higher than the min Capacity K_B^{min} defined through the So -called max allowable depth of discharge *DOD*, as in Equation (27), [55].

$$K_B^{min} \leq SOC_{B,h} \leq K_B^{max} \quad (26)$$

$$K_B^{min} = (1 - DOD) \times K_B^{max} \quad (27)$$

3.3.5. Constraints of Active Power

The relationship between the power generated by DGs with or without the utility grid (UG) and total demand at any point in time is as follows:

At connected mode;

$$\sum_{k=1}^{N_{DG}} P_{DG,k}(t) + P_{UG}(t) \pm P_{Batt}(t) = P_D(t) + P_{loss}(t) \quad (28)$$

At island mode;

$$\sum_{k=1}^{N_{DG}} P_{DG,k}(t) \pm P_{Batt}(t) = P_D(t) + P_{loss}(t) \quad (29)$$

Where P_{DG} is the real power generated of *DGs*, P_{UG} is the power supplied by the utility grid, P_{Batt} (t) is battery power when charging or discharging, P_D is the total real demand and P_{loss} is the total power loss.

3.3.6. Capacity of Generating

The hydropower and solar PV systems are modeled as variable power sources. Within a 24-hour period, the energy produced from each individual renewable energy source is managed between zero and its rated power. The restrictions can be stated as follows [56]:

$$0 \leq P_{PV} \leq P_{PV}^{max} \quad (30)$$

$$0 \leq P_{hydro} \leq P_{hydro}^{max} \quad (31)$$

4. Case study

In this study, OpenDSS software was used to analyze the rural distribution network (Al-Shajara feeder) shown in Fig.6 located in the village of Al-Shajara, southwest of the city of Kirkuk/Iraq. Geographically located at latitude 35°12.9' N and longitude 43°24.5' E. It is an 11 kV, 50 Hz radial distribution system. It contains ninety-three (93) buses, feeding agricultural and residential loads. The last bus (93) is 27 kilometers from the main substation. The highest average feeder load is 3,600 kW and 2,700 kVAr by direct measurement from the main substation and based on data from the control and communications department of the Electricity Distribution Company in Kirkuk. The main problems faced by rural distribution consumers are poor supply voltage, high system losses and unreliability.

The region has available water resource apart from the resource of solar energy, as the Tigris River flows along this region. Small projects to generate electricity by running water are complementary to projects to generate electricity by solar energy. When the solar radiation is high during the dry season, the water flow is low, and vice versa. Therefore, these resources were integrated with the distribution network to form a complementary source of electricity for the study site. In this case, 2500 kW solar PV panels and 3000 kW mini hydropower are used as the main energy sources. While 3850 kWh batteries are used as a backup due to the variable nature of renewable energies and to cover peak demand.

4.1. Average Seasonal Load Pattern

In this study an average hourly load profile during a year 2022 is considered**,** data of the control and communications department in Kirkuk Electricity Distribution Company was used to create 24 h load profiles for the loads. Based on the four seasons, four different types of load profiles were created (winter, spring, summer and fall). The months are divided into three-month groupings to establish the seasons. Winter: (December, January and February), spring: (March, April and May), summer: (June, July and August), fall: (September, October and November). The average of the active power for each hour during each season was used to produce the load profiles [57, 58]. The loads' power factors were 0.8, and using the active power demand and the power factors, it was possible to determine the reactive power demand. Data for 24 h each season are represented in the hourly average load pattern as shown in Figures 7 and 8.

To determine the active and reactive power load for every hour is obtain by following [37]:

$$P_L(t) = P_L\ peak \times Load\ \ pu(t) \quad (32)$$

$$Q_L(t) = Q_L\ peak \times Load\ \ pu(t) \quad (33)$$

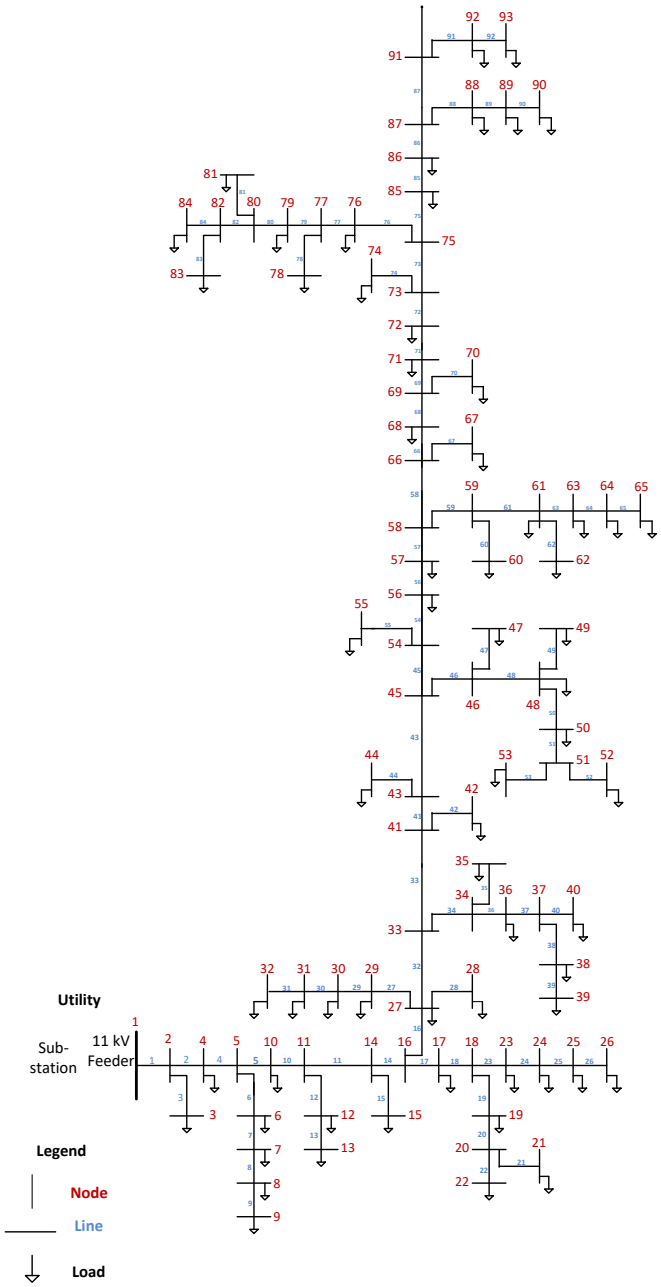

Fig. 6. Single line diagram of 11 kV Al-Shajara distribution network.

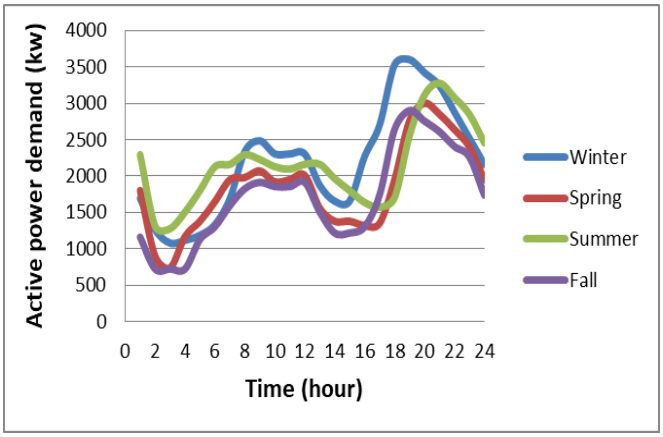

Fig. 7. The seasonal average hourly load pattern of the Al-Shajara feeder (kW).

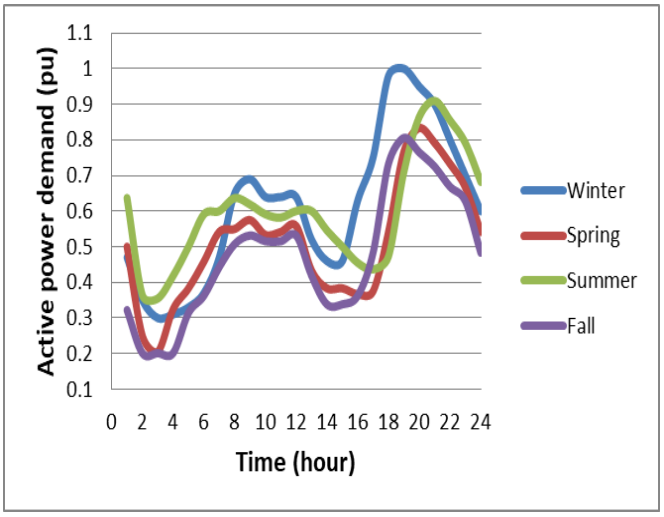

Fig. 8. Seasonal average hourly load pattern of the Al-Shajara feeder (pu).

With a few variations throughout the year, the power demand is consistent for the vast majority of loads. The winter and summer seasons typically see the highest usage. The fall and spring seasons saw the lowest levels of consumption.

4.2. Solar Radiation and Temperature

Hourly average temperature and solar radiation were used as input parameters in OpenDSS. Figures 9 and 10 show the solar radiation and temperature data for the study area obtained from "NASA POWER- Data Access Viewer" [59] and "Photoelectric Geographic Information System (PVGIS)" [60]. The greatest irradiation occurs in summer followed by spring and then autumn, and the least irradiation occurs in winter. The highest temperature occurs in summer, followed by autumn, spring and winter.

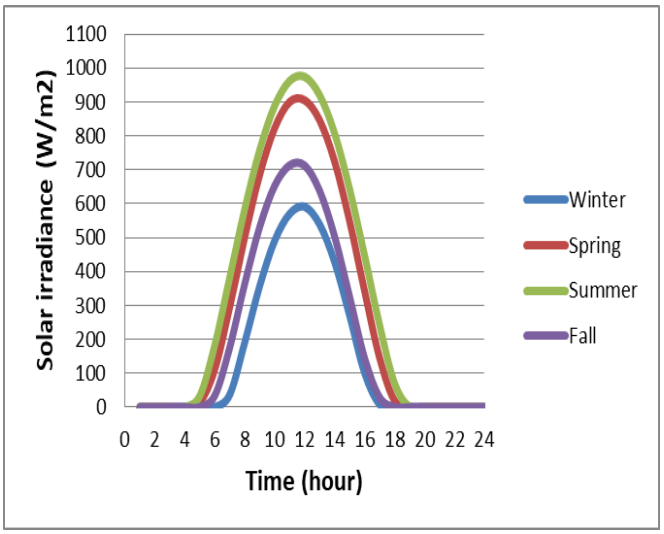

Fig. 9. seasonal hourly average solar radiation in the study area.

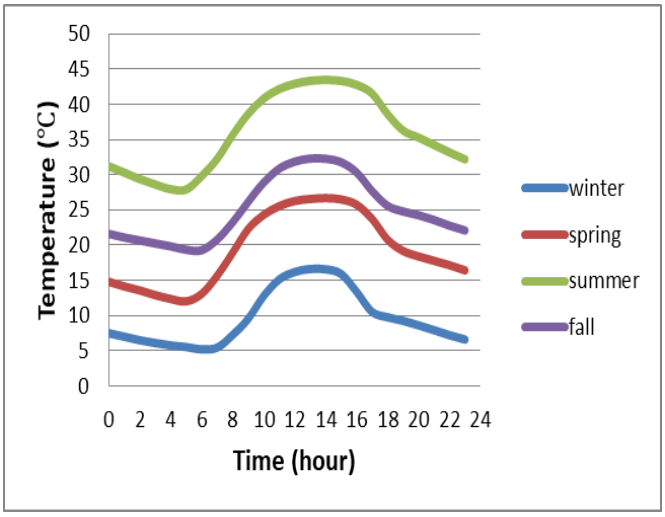

Fig. 10. Seasonal hourly average temperature in the study area, at 2 meters (°C).

5. Simulation Results and Discussions

5.1. Results of Power Flow Analysis of the system Before Integrating DGs and SCs

Power flow analysis of the actual system it shown in Fig.6 provides details on the system's voltage and branch loss based on the seasonal hourly load profile in Figures 7 and 8. Three different loads are considered in this work 3600 kW, 2161 kW and 725 kW, as follow:

- First load is at (19:00) in winter (3600 kW), which is the highest average load.
- Second load at (12:00) in the summer (2161 kW) equals 60% of the highest average load.
- Third load is at (3:00) in autumn (725 kW), which is the lowest average load.

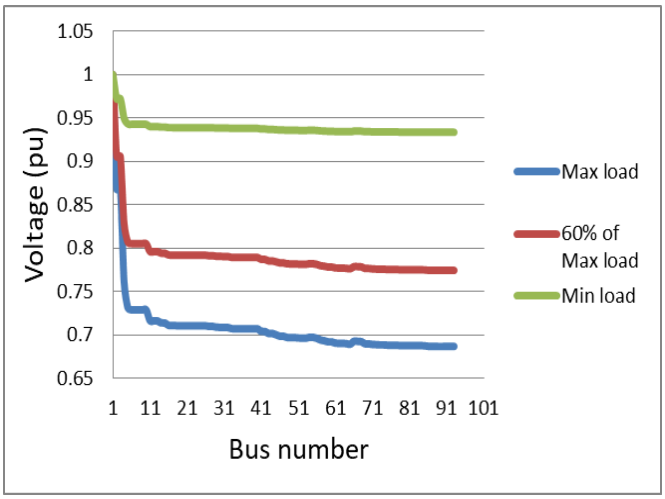

Fig. 11. Voltage profile of the system for three different loads, at base case before optimization.

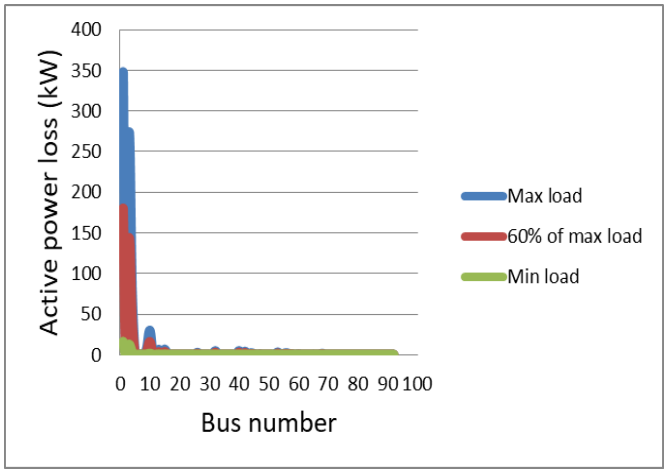

Fig. 12. Line loss of the system for three different loads, at base case before optimization kW.

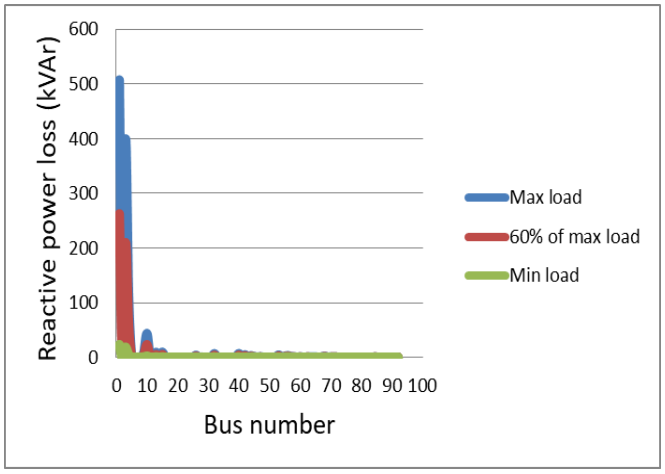

Fig. 13. Line loss of the system for three different loads, at base case before optimization kVAr.

Table 1. Results of power flow analysis of the Al-Shajara distribution network at base case for three different loads, 3600 kW, 2161 kW and 725 kW

Load (kW)	Load (kVAr)	Total losses (kW)	Total losses (kVAr)	Min voltage (pu) – Bus no	Max voltage (pu) – Bus no	Total voltage deviation TVD (pu)
3600	2700	779	1129	0.68666 - Bus 90	0.99996 - Bus 1	27.14155
2161	1620	406	589	0.77434 - Bus 90	0.99997 - Bus 1	19.52874
725	543	35	51	0.93361 - Bus 90	0.99999 - Bus 1	5.73892

5.2. Discussing the Results of Power Flow Analysis before Optimization

From the results of the power flow analysis presented in Table 1 and shown in Figures 11, 12 and 13 severe voltage drop of up to 0.68666 pu is shown, and the total power loss of the system is 21.65% of the total load. It turns out that the main problem in this network that we are studying is the excessive length of the transmission line, especially the starting lines, because the power loss and voltage drop mainly occurs between the first and fifth bus, which are the first three lines (1, 2 and 4). These lines are very long, its length is 18.661 km and is equal to 58% of the total length of the feeder, so it has very large impedance, which leads to energy loss and voltage drop.

90% of the power loss and 85% of the voltage drop occur in these three lines. We conclude from this that the power derived from the utility grid through this line must be reduced and nearby energy sources should be adopted to feed the loads of this network. The reason why the line is so long is that this area is remote and very far from power generation centers and power distribution substations. Therefore, we tried in this study to solve this problem and make this network completely or partially dispense with the energy derived from the utility grid, by installing distributed generators that adopt renewable energies, with the addition of shunt capacitors.

In this research, two proposed scenarios for improving the performance of the Al-Shajara distribution network will be studied.

- First scenario: improving the connected mode.
- Second scenario: improving the island mode.

In both scenarios the improving will be in terms of the voltage profile and reducing losses.

5.3. Selection of the Optimal Location for DGs and SCs on Al-Shajara Distribution Network

In this research, renewable energies are used to cover demand and improve energy quality, as the traditional radial network is transformed into a smart bidirectional network that can be controlled and can operate in connected and isolated mode. DGs should cover the total demand when the utility grid is isolated. Therefore, four SCs and seven DGs (photovoltaic power and mini-hydro power) with five battery pack are selected to cover the total demand. The number and size of generators are chosen according to the load and Capacity provided by each generator. As for the type of generators, they are chosen according to the study area and the resources available there. This network, which we are studying, is located in an area where water energy is available, an area adjacent to the Tigris River, in addition to solar energy, which is abundantly available in all regions of Iraq. Therefore, solar photovoltaic energy and hydroelectric energy are adopted as major resources in this work, and they are free resources in terms of operational cost compared to other energy sources. Batteries are added as an intermediate interface in order to address the problem of output fluctuations of photovoltaic systems and to meet the excessive demand for load at peak load. The optimum location for the DGs and SCs is chosen, using the (AutoAdd) algorithm. The AutoAdd algorithm is implemented through the OpenDSS program interfaced with MATLAB via the OpenDSS COM server.

Table 2. Optimum location and size of 7 DGs and 4 SCs on Al_Shajara distribution network

Type of DGs	Number of DGs	Total size	Location (Bus no)
Shunt Capacitor (SC)	4	$0 \le Q_{Sc} \le 2275$ kVAr (650, 650, 650, 325) kVAr	(57, 16, 85, 10)
Photovoltaic system (PV)	5	$0 \le P_{PV} \le 2500$ kW *UPF* (500, 500, 500, 500, 500) kW	(73, 61, 48, 16, 5)
Mini-Hydro Turbine (MHT)	2	$0 \le P_{MHT} \le 3000$ kW *PF* = 0.96 (1500, 1500) kW	(58, 58)
Battery pack	5	3850 kWh (770, 770, 770, 770, 770) kWh	(73, 61, 48, 16, 5)

5.4. Optimization Results and Discussions

The proposed technique is used to optimize the DGs and SCs in order to reduce total power losses and voltage drop of the system. System performance at three different loads through two scenarios, connected mode and island mode after integration of DGs and SCs, is shown as follows:

5.4.1. Optimization Results at Max Average Load

- Connected Mode

In this case a hydropower and batteries cover 84% of the demand, and 16% is covered by the utility grid, and PV cells do not generate power due to the absence of radiation in this hour. The minimum voltage on the network was 0.68666 pu and it is upgraded to 0.98451 pu, and the total losses of the system were 779 kW and 1129.45 kVAr, it has been reduced to 26.791 kW and 36.773 kVAr. Percentage reduction in total losses of real power, reactive power and total voltage deviation (TVD) are 96.56%, 96.74%, and 97.45% respectively.

- Island Mode

When the point of common connection (PCC) is opened (Bus1), the micro grid isolates itself and works in island mode. In the Isolated mode, DGs must provide all electrical demand without dependence on the main grid. Hydropower and batteries cover 100% of the demand, and PV cells do not generate power at this hour, the minimum voltage on the network was 0.68666 pu and it is upgraded to 0.9852 pu, and the total losses of the system were 779 kW and 1129.45 kVAr, it has been reduced to 21.8 kW and 29.7 kVAr. Percentage reduction in total losses of real power, reactive power and total voltage deviation (TVD) are 97.2%, 97.36% and 97.65% respectively.

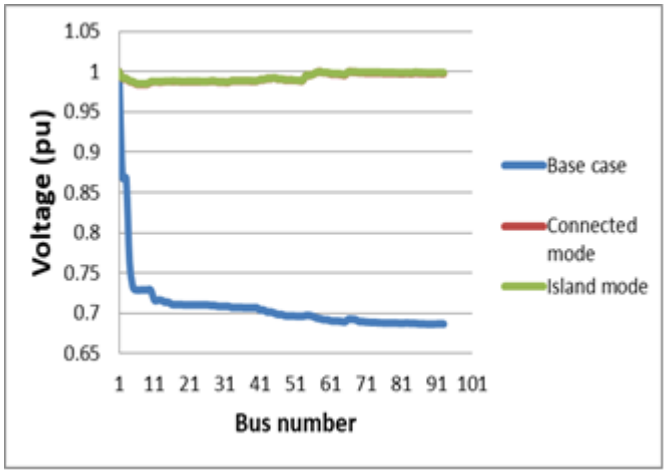

Fig. 14. Voltage profile of the system at load 3600 kW for different scenarios.

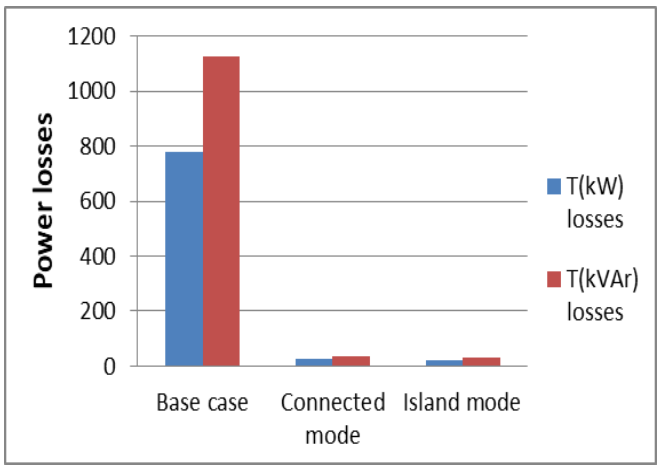

Fig. 15. Total power losses of the system at load 3600 kW for different scenarios.

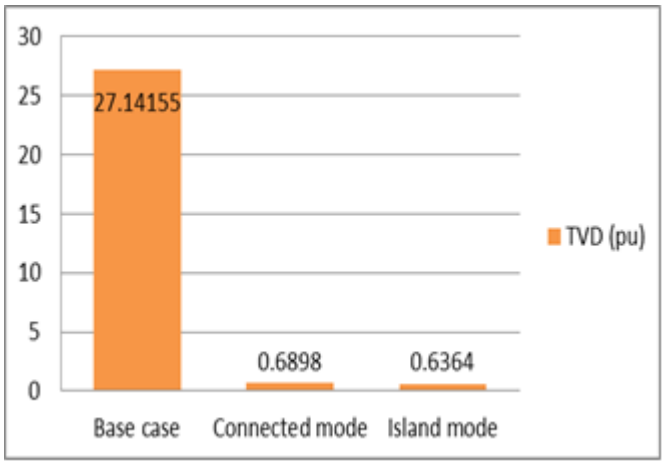

Fig. 16. Total voltage deviation (TVD) of the system at load 3600 kW for different scenarios.

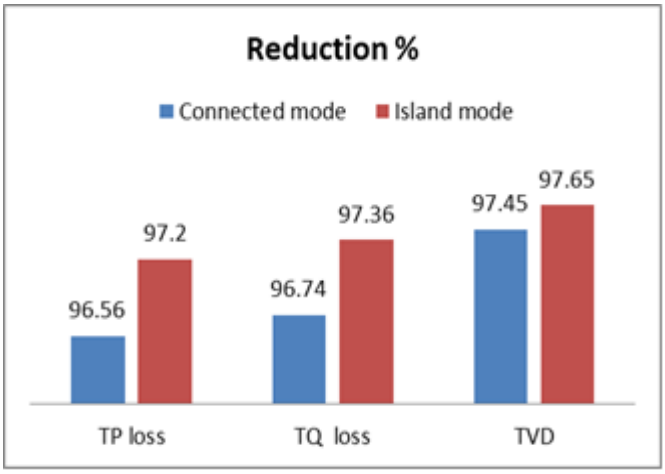

Fig. 17. Percentage reduction of system power losses and voltage deviation at load 3600 kW for two scenarios.

5.4.2. Optimization Results at 60% of the Max Average Load

- Connected Mode

In the case 60% of the max average load, photovoltaic systems cover 80% from demand, and utility grid cover 20%. The mini-hydro turbines are off and batteries are charging. The minimum voltage on the network was 0.77434 pu and it is upgraded to 0.98324 pu, and the total losses of the system were 406.72 kW and 589.7 kVAr, it has been reduced to 8.4 Kw and 11.6 kVAr. Percentage reduction in total losses of real power, reactive power and total voltage deviation (TVD) are 97.92%, 98.02% and 93.51% respectively.

- Island Mode

Photovoltaic systems cover 100% of the demand, and the mini-hydro turbines are off. The minimum voltage on the network was 0.77434 pu and it is upgraded to 0.9999 pu, and the total losses of the system were 406.72 kW and 589.7 kVAr, it has been reduced to 2.7 kW and 3.4 kVAr. Percentage reduction in total losses of real power, reactive power and total voltage deviation (TVD) are 99.32%, 99.42% and 101.87% respectively.

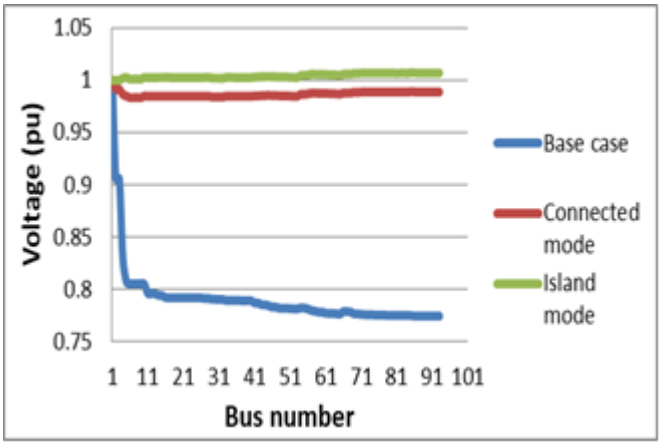

Fig. 18. Voltage profile of the system at load 2161 kW for different scenarios.

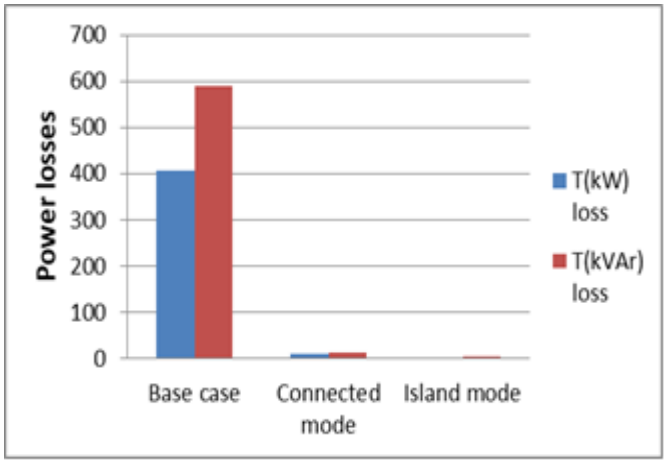

Fig. 19. Total power losses of the system at load 2161 kW for different scenarios.

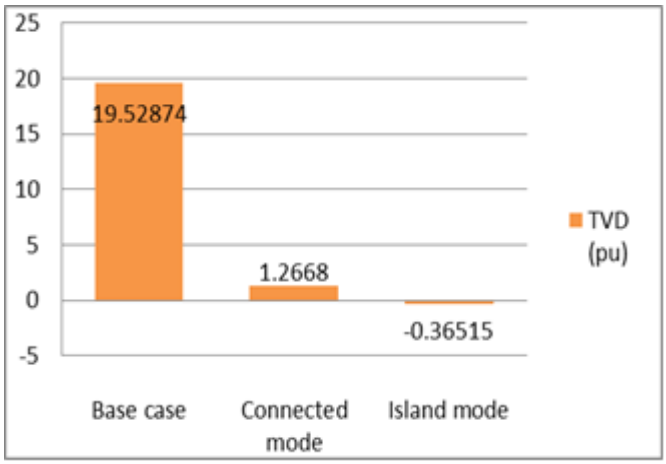

Fig. 20. Total voltage deviation (TVD) of the system at load 2161 kW for different scenarios.

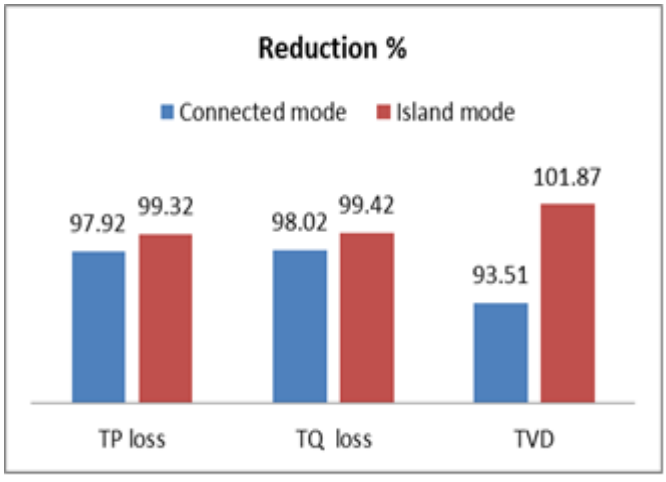

Fig. 21. Percentage reduction of system power losses and voltage deviation at load 2161 kW for two scenarios.

5.4.3. Optimization Results at Min Average Load

- Connected Mode

Hydropower covers 69% of the demand and 31% is covered by the utility grid. PV cells do not generate power due to the absence of irradiance in this hour and batteries are charging. The minimum voltage on the network was 0.93361 pu and it is upgraded to 0.99473 pu, and the total losses of the system were 35.7 kW and 51.76 kVAr, it has been reduced to 2.9 kW and 4.1 kVAr. Percentage reduction in total losses of real power, reactive power and total voltage deviation (TVD) are 91.85%, 92.03% and 94.27% respectively.

- Island Mode

Hydropower covers 100% of the demand and batteries are charging. PV systems do not generate power at this hour. The minimum voltage on the network was 0.93361 pu and it is upgraded to 0.99823 pu, and the total losses of the system were 35.7 kW and 51.76 kVAr, it has been reduced to 1.2 kW and 1.7 kVAr. Percentage reduction in total losses of real power, reactive power and total voltage deviation (TVD) are 96.47%, 96.65% and 98.75% respectively.

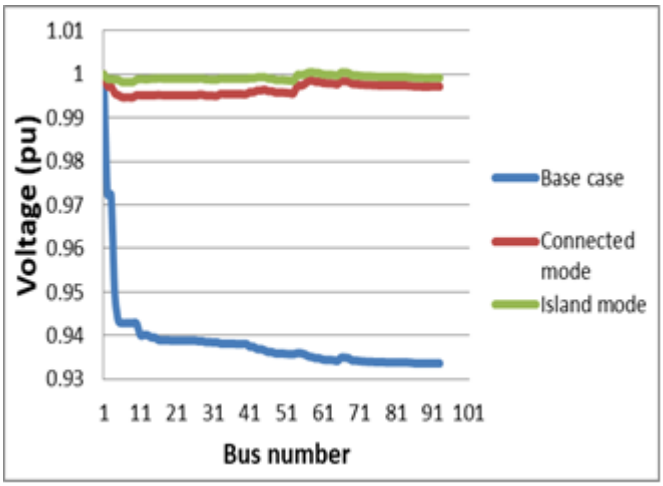

Fig. 22. Voltage profile of the system at load 725 kW for different scenarios.

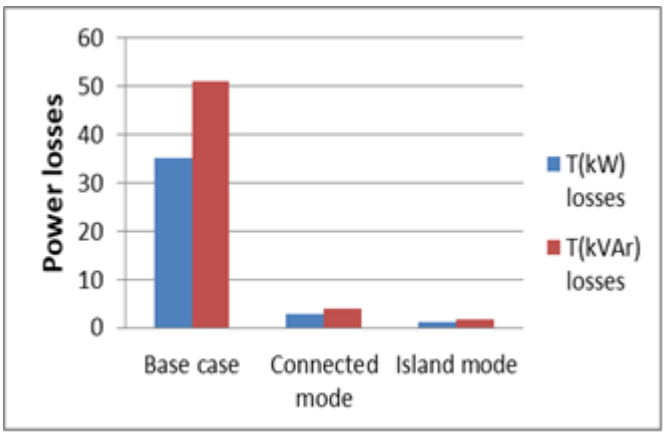

Fig. 23. Total power losses of the system at load 725 kW for different scenarios.

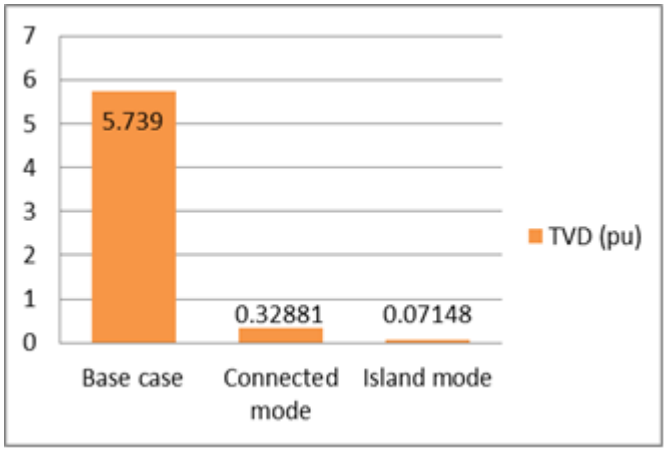

Fig. 24. Total voltage deviation (TVD) of the system at load 725 kW for different scenarios.

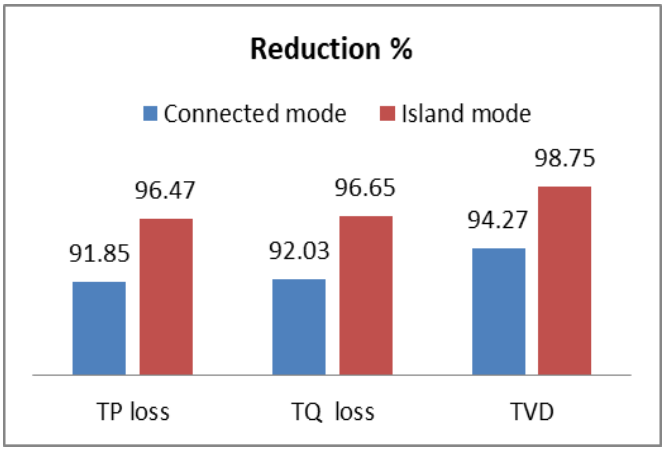

Fig. 25. Percentage reduction of system power losses and voltage deviation at load 725 kW for two scenarios.

Table 3. System performance parameters for all scenarios at three different loads

Parameters	Without DGs & SCs (Base case)			With DGs & SCs					
	Load 1	Load 2	Load 3	Load 1		Load 2		Load 3	
				Connected mode	Island mode	Connected mode	Island mode	Connected mode	Island mode
T P loss (kW)	779	406	35	26.791	21.8	8.4	2.7	2.9	1.2
T Q loss (kVAr)	1129	589	51	36.773	29.7	11.6	3.4	4.1	1.7
TVD (pu)	27.141	19.528	5.7389	0.6898	0.6364	1.2668	- 0.365	0.32881	0.0714
% reduction TP loss	--	--	--	96.56	97.2	97.92	99.32	91.85	96.47
% reduction TQ loss	--	--	--	96.74	97.36	98.02	99.42	92.03	96.65
% reduction TVD	--	--	--	97.45	97.65	93.51	101.87	94.27	98.75
Min voltage (pu) @ Bus no	0.6866 @ Bus 90	0.7743 @ Bus 90	0.9336 @ Bus 90	0.98451 @ Bus 8 & 9	0.9852 @ Bus 9	0.98324 @ Bus 8 & 9	0.9999 @ Bus 3	0.99473 @ Bus 7, 8& 9	0.9982 @ Bus 8 & 9
Max voltage (pu) @ Bus no	0.9999 @ Bus 1	0.9999 @ Bus 1	0.9999 @ Bus 1	1 @ Bus 1	1 @ Bus 1 & 58	1 @ Bus 1	1.0072 @ Bus 85	1 @ Bus 1	1.0005 @ Bus 58

5.4.4. Comparison between the Connected Mode and Island Mode Relative to the Base Case

Table 3 and the Figures (14-25) present a comparison between the connected mode and the island mode of Al-Shajara distribution network, in terms of power loss and voltage profile, at three different loads (3600, 2161 and 725) kW. The results show that the island mode is superior to the connected mode. The lowest voltage on the network in the island mode at the three loads respectively is 0.9852, 0.9999 and 0.99823 pu; against 0.98451, 0.98324 and 0.99473 pu in the connected mode. The active power losses at the three loads respectively are 21.8, 2.7 and 1.2 kW in island mode; against 26.791, 8.4 and 2.9 kW in connected mode. Also, for the reactive power loss and voltage deviation of the system in the island mode, it is less than in the connected mode.

6. Conclusions

This study aimed at the improvement of a power system by providing active and reactive power from DG and SC sources and their optimal allocation. By implementing the proposed optimization technique called AutoAdd to a real-time weak feeder on a purely conventional network as a case study substantially improved results. Where the penetration of distributed sources led to a significant reduction of power flow over long distances, thus it showed an improvement in the voltage level to be within the permissible limits in all buses and a significant reduction in energy losses for the both proposed scenarios at different loads, as the percentage of energy loss reduction reached 97% at full load. It was also found that the performance of the system in the island mode is better than in the connected mode in terms of the voltage level and the reduction of losses. Moreover, Table 3 presents the improvement results in detail.

We conclude from the results obtained from the analysis of power flow at three different loads before and after the integration of DGs and SCs show that the system performance improves as the power drawn from the utility grid decreases. This is due to the radial distribution and the distance of consumers from the energy source, and this requires providing nearby energy sources and dispensing with the energy supplied by the utility network, partially or completely (connected mode or island mode). As a result, reversing the direction of energy and selling the surplus from the microgrid's need to the utility grid through this long line is not feasible, because the transmitted energy will be of poor quality and lead to energy losses. Therefore, we exclude the option to sell energy. On this basis, the hybrid system is designed and the size and capacity of the distributed generators are chosen. However, the process of selling and exchanging energy between the microgrid and the utility grid will be positive if the power distribution station is available near Al-Shajara village in the future and the grid is reconfigured.

Acknowledgements

I extend my sincere thanks to my brother and teacher, Mustafa A. Kamoona.

References

[1] A. Oymak, M. Altun, F. Çakmak, S. Atiç, M. R. Tür, and R. Bayındir, "Distributed generation system planning based on renewable energy source", In 2022 10th International Conference on Smart Grid (icSmartGrid), IEEE, pp. 368-373, June 2022.

[2] A. Colmenar-Santos, C. Reino-Rio, D. Borge-Diez, and E. Collado-Fernández, "Distributed generation: A review of factors that can contribute most to achieve a scenario of DG units embedded in the new distribution networks", Renewable and Sustainable Energy Reviews, vol. 59, pp. 1130-1148, 2016.

[3] T. Adefarati, and R. C. Bansal, "Integration of renewable distributed generators into the distribution system: a review", IET Renewable Power Generation, vol. 10, No. 7, pp. 873-884, 2016.

[4] A. M. Colak, and O. Kaplan, "A review on the efficiency increment in a power system using smart grid technologies", In 2021 9th International Conference on Smart Grid (icSmartGrid), IEEE, pp. 192-196, June 2021.

[5] S. Guo, Q. Liu, J. Sun, and H. Jin, "A review on the utilization of hybrid renewable energy", Renewable and Sustainable Energy Reviews, vol. 91, pp. 1121-1147, 2018.

[6] S. Sinha, and S. S. Chandel, "Review of software tools for hybrid renewable energy systems", Renewable and sustainable energy reviews, vol. 32, pp. 192-205, 2014.

[7] A. Colak, and K. Ahmed, "A Brief Review on Capacity Sizing, Control and Energy Management in Hybrid Renewable Energy Systems", In 2021 10th International Conference on Renewable Energy Research and Application (ICRERA), pp. 453-458, September 2021.

[8] D. Akinyele, I. Okakwu, E. Olabode, R. Blanchard, T. Ajewole, and C. Monyei, "Integrated TEEP approach to microgrid design and planning with small hydro/solar/diesel resources for standalone application", e-Prime-Advances in Electrical Engineering, Electronics and Energy, vol. 2, p. 100091, 2022.

[9] C. Diyoke, L. E. Eja, and U. K. Chikwado, "Hydro Backed-up Hybrid Renewable System for Off-grid Power in Nigeria", American Journal of Electrical Power and Energy Systems, vol. 11, No. 2, pp. 31-47, 2022.

[10] S. K. Das, S. Sarkar, and D. Das, "Performance Enhancement of Grid-Connected Distribution Networks with Maximum Penetration of Optimally Allocated Distributed Generation Under Annual Load Variation", Arabian Journal for Science and Engineering, vol. 47, No. 11, pp. 14809-14839, 2022.

[11] M. A. Kamoona, O. C. Kivanc, and O. A. Ahmed, "Intelligent Energy Management System Evaluation of Hybrid Electric Vehicle Based on Recurrent Wavelet Neural Network and PSO Algorithm", International

Journal of Intelligent Engineering and Systems, vol. 16, no. 1, pp 388-401, 2023.

[12] M. A. Kamoona, O. C. Kivanc, and O. A. Ahmed, "Intelligent Energy Management System for Hybrid Electric Vehicle Based on Optimization Wavelet Neural Network by PSO Algorithm", In 12th International Conference on Information Systems and Advanced Technologies (ICISAT 2022) Intelligent Information, Data Science and Decision Support System", pp. 558-573, Cham: Springer International Publishing, February 2023.

[13] A. Eid, S. Kamel, H. M. Zawbaa, and M. Dardeer, "Improvement of active distribution systems with high penetration capacities of shunt reactive compensators and distributed generators using Bald Eagle Search", Ain Shams Engineering Journal, vol. 13, No. 6, p. 101792, 2022.

[14] N. R. Godha, V. N. Bapat, and I. Korachagaon, "Ant colony optimization technique for integrating renewable DG in distribution system with techno-economic objectives", Evolving Systems, vol. 13, No. 3, pp. 485-498, 2022.

[15] T. T. Nguyen, B. H. Dinh, T. D. Pham, and T. T. Nguyen, "Active power loss reduction for radial distribution systems by placing capacitors and PV systems with geography location constraints", Sustainability, vol. 12, No. 18, p. 7806, 2020.

[16] S. Adel, and C. Rachid, "Enhancement of a Voltage Drop in a Low-Voltage Grid by the Contribution of a Hybrid PV-Wind Turbine Generator", Journal of The Institution of Engineers (India): Series B, vol. 102, No. 5, pp. 947-956, 2021.

[17] A. S. Hassan, Y. Sun, and Z. Wang, "Multi-objective for optimal placement and sizing DG units in reducing loss of power and enhancing voltage profile using BPSO-SLFA", Energy Reports, vol. 6, pp. 1581-1589, 2020.

[18] E. E. Elattar, and S. K. Elsayed, "Optimal location and sizing of distributed generators based on renewable energy sources using modified moth flame optimization technique", IEEE Access, vol. 8, pp. 109625-109638, 2020.

[19] K. H. Truong, P. Nallagownden, I. Elamvazuthi, and D. N. Vo, "An improved meta-heuristic method to maximize the penetration of distributed generation in radial distribution networks", Neural Computing and Applications, vol. 32, pp. 10159-10181, 2020.

[20] R. K. Samala, and M. R. Kotapuri, "Optimal allocation of distributed generations using hybrid technique with fuzzy logic controller radial distribution system", SN Applied Sciences, vol. 2, No. 2, p. 191, 2020.

[21] S. Ouali, and A. Cherkaoui, "Optimal allocation of combined renewable distributed generation and capacitor units for interconnection cost reduction", Journal of Electrical and Computer Engineering, vol. 2020, pp. 1-11, 2020.

[22] R. C. Dugan, and T. McDermott, "The Open Distribution System Simulator (OpenDSS)", EPRI, Reference guide, 2016.

[23] F. M. Camilo, V. F. Pires, R. Castro, and M. E. Almeida, "The impact of harmonics compensation ancillary services of photovoltaic microgeneration in low voltage distribution networks", Sustainable cities and society, vol. 39, pp. 449-458, 2018.

[24] N. Eltawil, M. Sulaiman, M. Shamshiri, and Z. Bin Ibrahim, "Optimum allocation of capacitor and DG in MV distribution network using PSO and opendss", ARPN J. Eng. Appl. Sci, vol. 14, No. 2, pp. 363-371, 2019.

[25] I. J. Hasan, C. K. Gan, M. Shamshiri, M. R. Ab Ghani, and R. B. Omar, "Optimum feeder routing and distribution substation placement and sizing using PSO and MST", Indian Journal of Science and Technology, vol. 7, No. 10, pp. 1682-1689, 2014.

[26] S. Pukhrem, M. F. Conlon, K. Sunderland, and M. Basu, "Analysis of voltage fluctuation and flicker on distribution networks with significant PV installations", in 31st European Photovoltaic Solar Energy Conference and Exhibition (EU PVSEC), 2015.

[27] C. Liang, H. Jun, W. Yiran, T. Jian, L. Hong, G. Sanrong, and W. Yin, "Analysis of access location and capacity of distributed generation based on OpenDSS", 2018 IEEE China International Conference on Electricity Distribution (CICED), pp. 2264-2268, September 2018.

[28] J. Han, J. Huang, Y. Wu, H. Liu, Z. Xie, H. Huang, and S. Gui, "Research on Optimal Access Location and Capacity of MultiStage Multi-Scenario Distributed Power Supply Based on OpenDSS", IOP Conference Series: Earth and Environmental Science, vol. 300, no. 4, p. 042036, July 2019.

[29] S. Nie, X. P. Fu, P. Li, F. Gao, C. D. Ding, H. Yu, and C. S. Wang, "Analysis of the impact of DG on distribution network reconfiguration using OpenDSS", IEEE PES Innovative Smart Grid Technologies, pp. 1-5, May 2012.

[30] P. Prabpal, Y. Kongjeen, and K. Bhumkittipich, "Optimal Battery Energy Storage System Based on VAR Control Strategies Using Particle Swarm Optimization for Power Distribution System", Symmetry, vol. 13, no. 9, p. 1692, 2021.

[31] Zhang, C.X. and Zeng, Y, "Voltage and reactive power control method for distribution grid", In 2013 IEEE PES Asia-Pacific Power and Energy Engineering Conference (APPEEC), pp. 1-6, 2013.

[32] S. Singh, D. Shukla, and S. P. Singh, "Peak demand reduction in distribution network with smart grid-enabled CVR", in 2016 IEEE Innovative Smart Grid

Technologies-Asia (ISGT-Asia), pp. 735-740, November 2016.

[33] K. Sredenšek, B. Štumberger, M. Hadžiselimović, S. Seme, and K. Deželak, "Experimental validation of a thermo-electric model of the photovoltaic module under outdoor conditions", Applied Sciences, vol. 11, no. 11, p. 5287, 2021.

[34] A. S. Aziz, M. F. N. Tajuddin, T. E. K. Zidane, C. L. Su, A. J. K. Alrubaie, and M. J. Alwazzan, "Techno-economic and environmental evaluation of PV/diesel/battery hybrid energy system using improved dispatch strategy", Energy Reports, vol. 8, pp. 6794-6814, 2022.

[35] L. S. Pantic, T. M. Pavlović, D. D. Milosavljević, I. S. Radonjic, M. K. Radovic, and G. Sazhko, "The assessment of different models to predict solar module temperature, output power and efficiency for Nis, Serbia", Energy, vol. 109, pp. 38-48, 2016.

[36] C. Li, S. V. Spataru, K. Zhang, Y. Yang, and H. Wei, "A multi-state dynamic thermal model for accurate photovoltaic cell temperature estimation", IEEE Journal of Photovoltaics, vol. 10, no. 5, pp. 1465-1473, 2020.

[37] S. Barik, and D. Das, "Determining the sizes of renewable DGs considering seasonal variation of generation and load and their impact on system load growth", IET Renewable Power Generation, vol. 12, no. 10, pp. 1101-1110, 2018.

[38] E. Kymakis, S. Kalykakis, and T. M. Papazoglou, "Performance analysis of a grid connected photovoltaic park on the island of Crete", Energy conversion and management, vol. 50, no. 3, pp. 433-438, 2009.

[39] E. P. J. A. Skoplaki, and J. A. Palyvos, "Operating temperature of photovoltaic modules: A survey of pertinent correlations", Renewable energy, vol. 34, no.1, pp. 23-29, 2009.

[40] Ministry of water resources Iraq. Available: "https://mowr.gov.iq/2021/05/25/%D9%88%D8%B2%D9%8A, Accessed February 2023".

[41] S. S. Abdallah, B. A. D. R. Ali, and M. M. Ahmed, "Study of Geometric Elements for the Proposed Protecting Dam Reservoir in Al-Fat'ha Area, Iraq", in E3S Web of Conferences, EDP Sciences, vol. 318, p. 01009, 2021.

[42] غسان شعلان ندا الشاهري, and صبار عبدالله صالح, "أستتباع الفيضان لنهر دجلة في بيجي وخزان سد مكحول المقترح بتشغيل افتراضي للسد", Tikrit Journal of Pure Science, vol. 22, no. 1, pp. 115-127, 2018.

[43] P. Dusenge, J. D. A. Niyonsaba, J. D. D. Samvura, J. Bikorimana, T. Rwahama, and E. Mudaheranwa, "feasibility study of hybrid Hydro-PV power plant possible deployment in remote rural area", In 2022 IEEE PES/IAS PowerAfrica, pp. 1-5, August 2022.

[44] S. Zeb, M. Ali, A. Mujeeb, and H. Ullah, "Cost efficient Mini hydro plant with low water head whirlpool design methodology for rural areas: Micro Hydro Whirlpool power plant", In 2019 2nd International Conference on Computing, Mathematics and Engineering Technologies (iCoMET), IEEE, pp. 1-7, January 2019.

[45] E. I. Okhueleigbe, and O. Godswill, "Mini-hydro turbine: solution to power challenges in an emerging society with abundance of water", American Journal of Engineering and Technology Management, vol. 2, no. 2, pp. 7-12, 2017.

[46] A. Oymak, and M. R. Tur, "A Short Review on the Optimization Methods Using for Distributed Generation Planning", International Journal of Smart Grid-ijSmartGrid, vol. 6, no. 3, pp. 54-64, 2022.

[47] R. V. Agila, D. Icaza, and J. González, "Optimization of the use and Exploitation of the Water Resource of the Catchments of the" Hydroelectric Power Plant Ing. Carlos Mora Carrion" located in the Canton of Zamora", In 2020 9th International Conference on Renewable Energy Research and Application (ICRERA), pp. 526-531, IEEE, September 2020.

[48] M. M. Kamal, I. Ashraf, and E. Fernandez, "Efficient two-layer rural electrification planning and techno-economic assessment integrating renewable sources", Energy Storage, vol. 4, no. 3, p. e314, 2022.

[49] A. Hassan, Y. M. Al-Abdeli, M. Masek, and O. Bass, "Optimal sizing and energy scheduling of grid-supplemented solar PV systems with battery storage: Sensitivity of reliability and financial constraints", Energy, vol. 238, p. 121780, 2022.

[50] A. Fathy, K. Kaaniche, and T. M. Alanazi, "Recent approach based social spider optimizer for optimal sizing of hybrid PV/wind/battery/diesel integrated microgrid in Aljouf region", IEEE Access, vol. 8, pp. 57630-57645, 2020.

[51] S. Moghaddam, M. Bigdeli, M. Moradlou, and P. Siano, "Designing of stand-alone hybrid PV/wind/battery system using improved crow search algorithm considering reliability index", International Journal of Energy and Environmental Engineering, vol. 10, no. 4, pp. 429-449, 2019.

[52] T. T. Nguyen, B. H. Dinh, T. D. Pham, and T. T. Nguyen, "Active power loss reduction for radial distribution systems by placing capacitors and PV systems with geography location constraints", Sustainability, vol. 12, no. 18, p. 7806, 2020.

[53] M. G. Hemeida, S. Alkhalaf, A. A. A. Mohamed, A. A. Ibrahim, and T. Senjyu, "Distributed generators optimization based on multi-objective functions using manta rays foraging optimization algorithm (MRFO)", Energies, vol. 13, no.15, p. 3847, 2020.

[54] A. Eid, "Allocation of distributed generations in radial distribution systems using adaptive PSO and modified GSA multi-objective optimizations", Alexandria Engineering Journal, vol. 59, no. 6, pp. 4771-4786, 2020.

[55] M. Bortolini, M. Gamberi, and A. Graziani, "Technical and economic design of photovoltaic and battery energy storage system", Energy Conversion and Management, vol. 86, pp. 81-92, 2014.

[56] O. Dzobo, "Optimal power dispatch of an off-grid renewable energy-based system using linear programming", in 2022 57th International Universities Power Engineering Conference (UPEC), IEEE, pp. 1-5, August 2022.

[57] M. Z. ul Abideen, O. Ellabban, S. S. Refaat, H. Abu-Rub, and L. Al-Fagih, "A novel methodology to determine the maximum PV penetration in distribution networks", in 2019 2nd International Conference on Smart Grid and Renewable Energy (SGRE), IEEE, pp. 1-6, November 2019.

[58] S. Kenu, R. Uhunmwangho, and K. Okedu, "Harnessing Solar and Wind Power for Hybrid Stand-alone Energy System: The Case of Coastline Communities in Delta State of Southern Nigeria", International Journal of Smart Grid-ijSmartGrid, vol. 7, no. 1, pp. 25-37, 2023.

[59] Power Data Access Viewer NASA. Available: "https://power.larc.nasa.gov/data-access-viewer/, Accessed March 2023".

[60] Photovoltaic Geographical Information System. Available: "https://re.jrc.ec.europa.eu/pvg_tools/en/#DR, Accessed March 2023".